# Gas and Drop Behavior in Reacting and Non-Reacting Air-Blast Atomizer Sprays

Vincent G. McDonell* and Scott Samuelsen†
*University of California, Irvine, Irvine, California 92717*

**A detailed study of the two-phase flow produced by a gas-turbine air-blast atomizer is performed with the goal of identifying the interaction between the two phases for both non-reacting and reacting conditions. A two-component phase Doppler interferometry is utilized to characterize three flowfields produced by the atomizer: 1) the single-phase flow, 2) the two-phase non-reacting spray, and 3) the two-phase reacting spray. Measurements of the mean and fluctuating axial and azimuthal velocities for each phase are obtained. In addition, the droplet size distribution, volume flux, and concentration are measured. The results reveal the strong influence of the dispersed phase on the gas, and the influence of reaction on both the gas and the droplet field. The presence of the spray significantly alters the inlet condition of the atomizer. With this alteration quantified, it is possible to deduce that the inertia associated with the dispersed phase damps the fluctuating velocities of the gas. Reaction reduces the volume flux of the droplets, broadens the local volume distribution of the droplets in the region of the reaction zone, increases the axial velocities and radial spread of the gas, and increases the anisotropy in the region of the reaction zone.**

## Introduction

DETAILED measurements of both the continuous and dispersed phases in liquid fuel sprays are necessary to develop 1) an understanding of the physical processes of evaporation, mixing, and momentum and mass exchange, and 2) a data base for the verification and development of computational codes.

Further, measurements in both non-reacting and reacting sprays are of interest. Studies in the absence of reaction provide a baseline to assess the impact of reaction. Likewise, a data base can be established that utilizes the same geometry, but provides information with and without the complexity of chemical reaction.

Optical measurements of droplet size in reacting sprays have been made previously (e.g., Refs. 1–4). Although these studies have been useful in demonstrating the application of various optical techniques to the measurement of drop size in reacting sprays, the necessary gas phase data are not provided.

Of the diagnostics available, phase Doppler interferometry has the potential for providing the needed data for both the continuous phase and dispersed phase (e.g., Refs. 5–8). Of the above studies employing phase Doppler in reacting flows,[1–3] single-component instruments were utilized. In sprays featuring atomization or aerodynamically induced swirl, two or three significant velocity components can be induced in both the continuous and dispersed phases. In such cases, non-biased phase Doppler results may require a simultaneous two-component measurement. Other issues also limit the use of these data in developing an understanding of the physics, or in developing a data base for a numerical code challenge. For example, in these studies:

1) Data were acquired in the absence of a detailed survey of atomizer symmetry. Hence, the effect of asymmetries on the data sets is unknown.

2) The liquids used were multicomponent fuels. Hence, the use of the data for modeling is limited.

3) In the cases where non-reacting sprays are compared with reacting sprays in a model swirl-stabilized model combustor,[1,2] data acquired in the absence of reaction were also in geometries free of both confinement and a dome swirler. Hence, the effect of reaction alone was not isolated.

The present study characterizes, in the absence and presence of reaction, the gas and drops in a spray produced by a production air-blast atomizer. Measurements are made using two-component phase Doppler interferometry.[5] A single-component fuel (methanol) with properties desirable for modeling is used.

Previous studies of the same atomizer and spray have examined the role of the two phases in establishing the symmetry of the spray field[9] and demonstrated the extension of the diagnostic employed to reacting environments.[10] These results are useful in establishing the capability of the instrumentation in characterizing two-phase polydispersed flows and in characterizing sprays under reacting conditions. The initial data acquired in the present effort were previously presented.[10] The focus of that paper was on establishing the performance of the diagnostics under reacting as well as non-reacting conditions. The acquisition of additional and redundant data and analysis of all the data have now been completed, and the results are presented in this paper, with emphasis upon the physical mechanisms occurring in the reacting and non-reacting sprays.

## Approach

The approach taken is to carefully characterize the two-phase flow produced by a practical air-blast atomizer by acquiring the measurements of mean and fluctuating axial and azimuthal velocities for each phase, and the measurements of size and volume flux of the dispersed phase. The single-phase flow (i.e., "atomizing" air only through the atomizer, in the absence of liquid) is initially characterized. Next, liquid methanol is injected in the presence of atomizing air, and the resulting two-phase flow is characterized. Finally, the spray is ignited, and the reacting flow is characterized in the same manner. The tests are run at 1 atm, and all air used is introduced at 18–21° C. Measurements are obtained at three axial locations, $Z$ = 50, 75, and 100 mm.

Received Dec. 11, 1989; revision received June 28, 1990; accepted for publication Sept. 12, 1990. 

*Graduate Researcher, Institute for Combustion and Propulsion Science and Technology. Student Member AIAA.

†Professor of Mechanical and Environmental Engineering, Institute for Combustion and Propulsion Science and Technology. Member AIAA.

## Experiment

### Atomizer

The air-blast atomizer utilized in the present study is shown in Fig. 1. The atomizer is used commercially in small-scale gas-turbine engines. The atomizer is operated at an air-to-fuel ratio of 1.0, with a fuel mass flow of 0.00203 kg/s. Methanol is employed for three reasons: at the ambient condition used, 1) it will readily vaporize, 2) the vapor has approximately the same density as air, and 3) the liquid saturation temperature (−10°C) can be easily achieved prior to atomization, ensuring that thermal gradients within the droplets are minimized. Although selected for use based on non-reacting conditions, methanol is also suitable for reacting conditions. Table 1 summarizes the characteristics of the selected operating conditions. The effective area, $A_{cd}$, is determined from the pressure drop across the atomizer and the air mass flow rate.[11] For the relatively low-pressure drops of the present study, the air flow is approximately incompressible, and the effective area can be used to establish the bulk velocity of the air exiting the atomizer.

It is also necessary to know the air flow through each passage of the atomizer. A study was conducted to quantify the flow split, and it was found that an approximately even split occurs for the present operating condition.

### Facility

The facility utilized is shown in Fig. 2. The test article is oriented downward, suspended from a traverse providing motion in the axial direction. This traverse is attached to a support structure, which is, in turn, suspended from the optical table by a two-dimensional traverse system, thus providing three degrees of translational freedom. In addition, the test article may be rotated about the centerline to provide one rotational degree of freedom. The support structure is enclosed to provide a 455 × 455 mm duct. Optical access is provided by 3 mm thick 75 × 300 mm vycor sheets. The exhaust system is designed for reacting and non-reacting conditions. The system provides a bulk air velocity of 1 m/s (with no atomizer flows) through the square duct in the present study. A vibrated fluidized bed seeder feeds a minifold at the inlet to the duct to provide the information for the gas phase. $Al_2O_3$ (nominally 1.0 $\mu$m) mixed with 3% $SiO_2$ (a flow agent to reduce agglomeration that minimizes fluctuations in fluidization rate) is used to seed the flow.

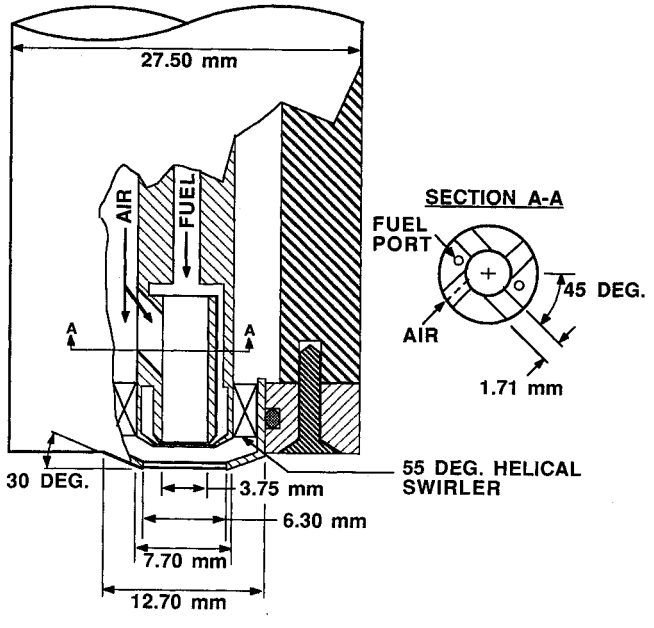


**Fig. 1 Air-blast atomizer and fixture used to supply air and fuel.**

**Table 1 Operational characteristics of air-blast atomizer**

| Air flow, gms/s | Air $\Delta P$, kPa | $A_{cd}$,[a] m$^2$ | Fuel flow, gms/s | Fuel $\Delta P$, kPa |
|---|---|---|---|---|
| 2.03 | 3.5 | $2.32 \times 10^{-5}$ | 0.00 | 0.0 |
| 2.03 | 4.75 | $2.00 \times 10^{-5}$ | 2.03 | 83.5 |

[a]Based on Textron Turbo Component methodology.[11]

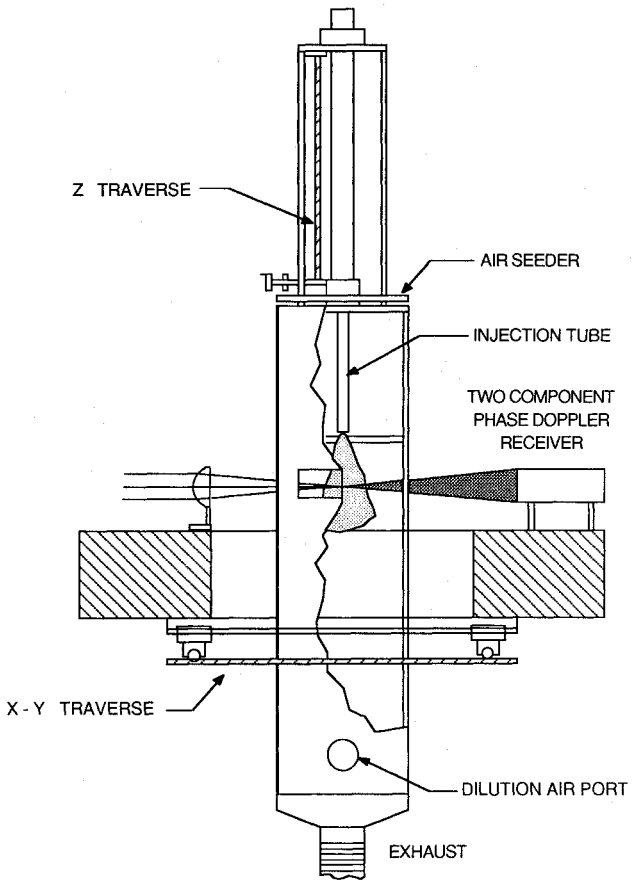


**Fig. 2 Facility.**

It was found that seeding the atomizing air streams led to a gradual buildup of seed on the atomizer swirl vanes that, after approximately one hour, began to change the aerodynamic flowfield produced. Further studies directed at this problem revealed that, at the locations of the measurements reported here, the measured mean and fluctuating velocities did not significantly change when not seeding the atomizing air. This is due to the considerable mixing and entrainment of surrounding air by the 50 mm axial location. As a result, only the coflowing duct air was seeded in the present study.

### Diagnostics

A two-component phase Doppler interferometer (Aerometrics, Inc. Model 2100-3; system clock: 80 MHz) is utilized to characterize the flows of interest. A schematic of the optical arrangement used is shown in Fig. 3. Two orthogonal sets of fringes are provided by separating the 488.0 and 514.5 nm lines from an $Ar^+$ laser. In addition, the planes of polarization of the beams forming each probe are orthogonal. The receiver unit utilizes both polarization and chromatic separation of the signals to reduce "cross talk" to a minimum. Data acquisition, processing, and storage are controlled by an IBM AT computer. Details of the principle for measuring the size and velocity of individual drops, as well as for volume flux, are given elsewhere.[12,13] The results presented are based on statistics associated with averages of individual events.

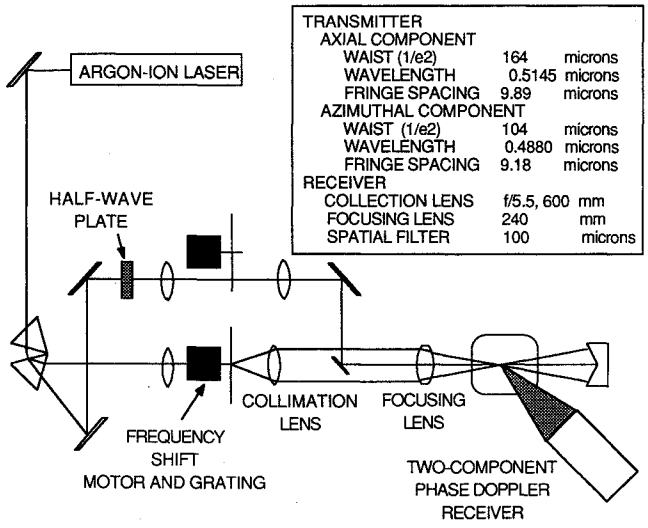


**Fig. 3 Diagnostics.**

The technique is well-suited to reacting flows because the phase shift measurement is relatively insensitive to the flame.[5] The technique is, however, susceptible to errors, due to beam steering. The size of the present flame is small enough to result in only small errors from this effect. Based upon sensitivity studies, the primary errors due to beam steering are a decrease in counting efficiency and an elevated fluctuating velocity.[14] In the relatively small reaction zone of the present study, these errors are considered small. Maximum error due to temperature dependent liquid refractive index is 3.3% (based on using 134 at 0°C and 1.31 at 64.7°C, where the indices are determined via the Eykman relationship).

Discrimination of phases is inherent in the operation of the instrument. By seeding the flow, optimizing the sensitivity of the instrument to small particles, sizing all particles, and then extracting the particles that are small enough to track the flow (particles less than 4 $\mu$m in diameter are used in this study), the velocity of the gas phase within the spray may be deduced. This approach has been applied successfully using dry powders as seed in monodispersed particle laden jets (e.g., Refs. 6 and 7), and using both powders and mists in polydispersed sprays (e.g., Refs. 8, 9 and 15). Although the powder (alumina, in this case) is not spherical, the small particle produces a small phase shift that the instrument interprets as a small spherical particle. Of course, the validation rate is reduced when using either powders or mists relative to the case where sizing is not employed. Studies were conducted to verify that the instrument interpreted the $Al_2O_3$ as a small particle. This approach works well in the present flow, but may be hindered by high concentrations of large drops, low-quality optical access, and with lower power lasers.

Based on repetition of measurements at various points in the sprays, errors in the means of size distribution are estimated at $\pm 1$ $\mu$m, and $\pm 0.25$ m/s for the mean velocity. Errors associated with the flux measurement are difficult to establish, because of the large number of parameters involved in the calculation of this value. This will be discussed in more detail in the following section.

## Results and Discussion

Results are presented first for the continuous (gas) phase flow for the following three cases: without the spray and with the non-reacting and reacting spray. Next, results for the dispersed phase spray are presented for the two-phase flow for the following two conditions: non-reacting and reacting spray. Figure 4 presents a schematic of the spray structure for these two cases.

### Continuous Phase

Figure 5 presents the axial continuous phase (i.e., gas) velocities. In general, the mean axial gas velocities are increased

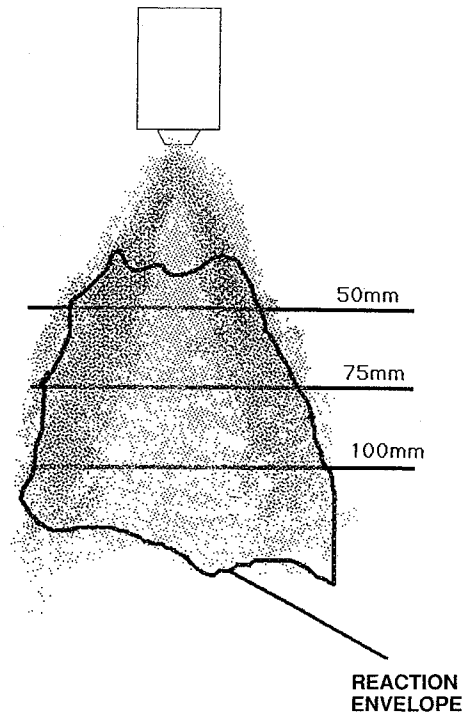


**Fig. 4 Schematic of spray structure.**

by the presence of the non-reacting spray for reasons now discussed.

When the liquid is present, two factors are involved that change the gas velocity with respect to the single-phase case. First, due to a change in the inlet condition, the initial velocities at the exit plane of the atomizer are *increased* by 16% (based upon the change in atomizer $A_{cd}$ shown in Table 1). The measured velocities of the gas in the field of the spray do not show this much increase. This is attributed to the second factor, energy transfer from the air to the droplets during liquid breakup and acceleration of the drops, which *reduces* the velocity of the air.

When the spray is ignited, at $Z = 50$ mm, the reaction is just getting started, and relatively little influence on the axial velocity is observed. By $Z = 75$ and 100 mm, the gas has expanded, giving rise to a significant increase in axial velocities.

Figure 5 also presents the *rms* fluctuation of the axial velocity about the mean for the three cases. The presence of the dispersed phase under non-reacting conditions reduces the fluctuation of the axial velocity at all axial stations. The decrease in turbulence is consistent with a reduction in the decay of the mean axial velocity. (From $Z = 50$ to $Z = 100$ mm, the centerline velocity decreases by 30% and 25% for the single- and two-phase cases, respectively.) When the spray is ignited, the effect on turbulence at $Z = 50$ mm is minor, as is the effect on mean axial velocity. By $Z = 75$ and 100 mm, reaction increases the magnitude of the axial velocity fluctuations about the mean to levels greater than or equal to those for the non-reacting case. The regions where a significant increase in the magnitude of the fluctuating velocities is observed (15–40 mm from the centerline) correspond to regions into which the gases have expanded, as indicated by the mean velocity profiles.

Examination of the azimuthal velocity component (shown in Fig. 6) reveals that the presence of the spray does not significantly impact the amount of swirl in the gas phase. In general, the magnitude of the azimuthal velocities are quite small, and, given the error in the velocity measurement, any apparent differences for the three cases are not significant. It is noted that the aerodynamic centerline of the flow moves away from centerline when the reacting spray is present. Previous work has demonstrated that practical atomizers, in gen-

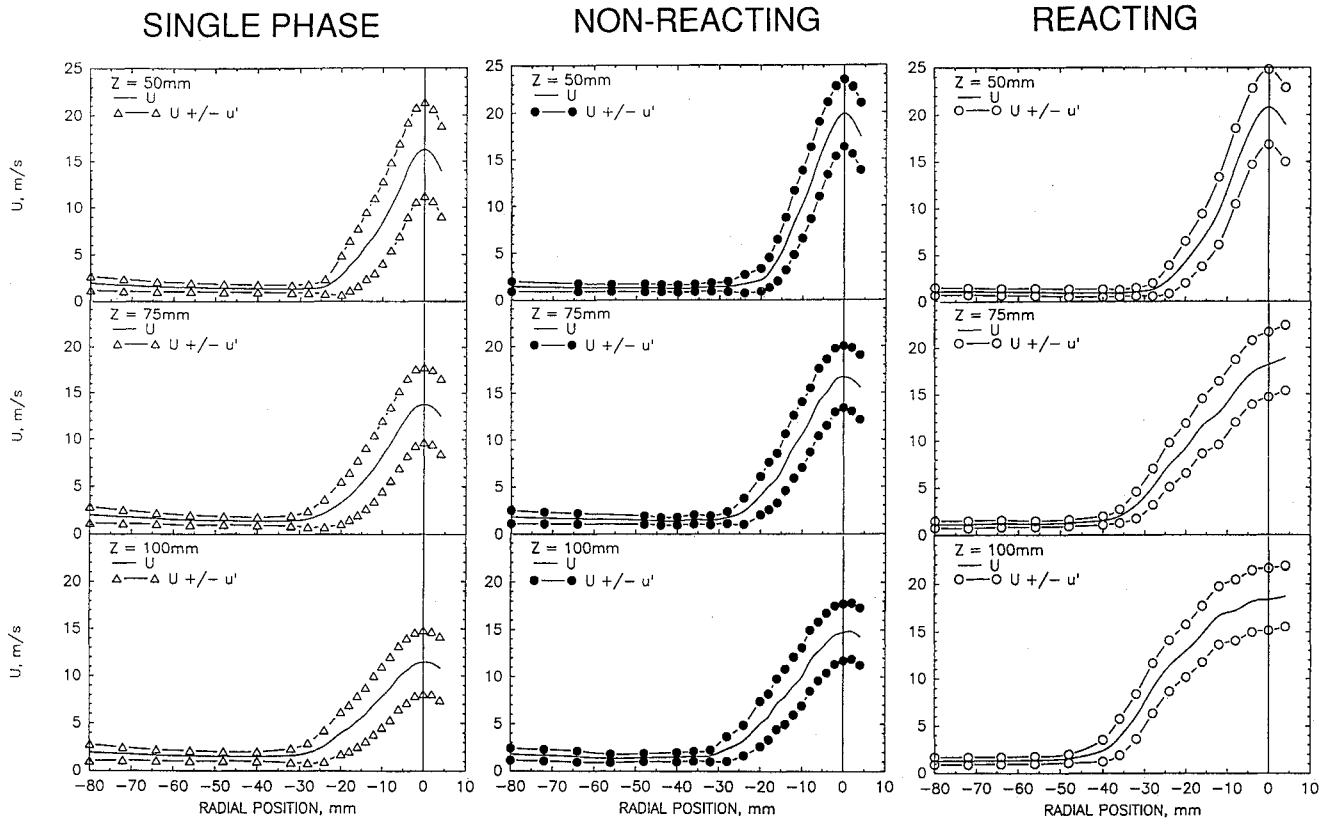


**Fig. 5 Continuous phase axial velocities.**

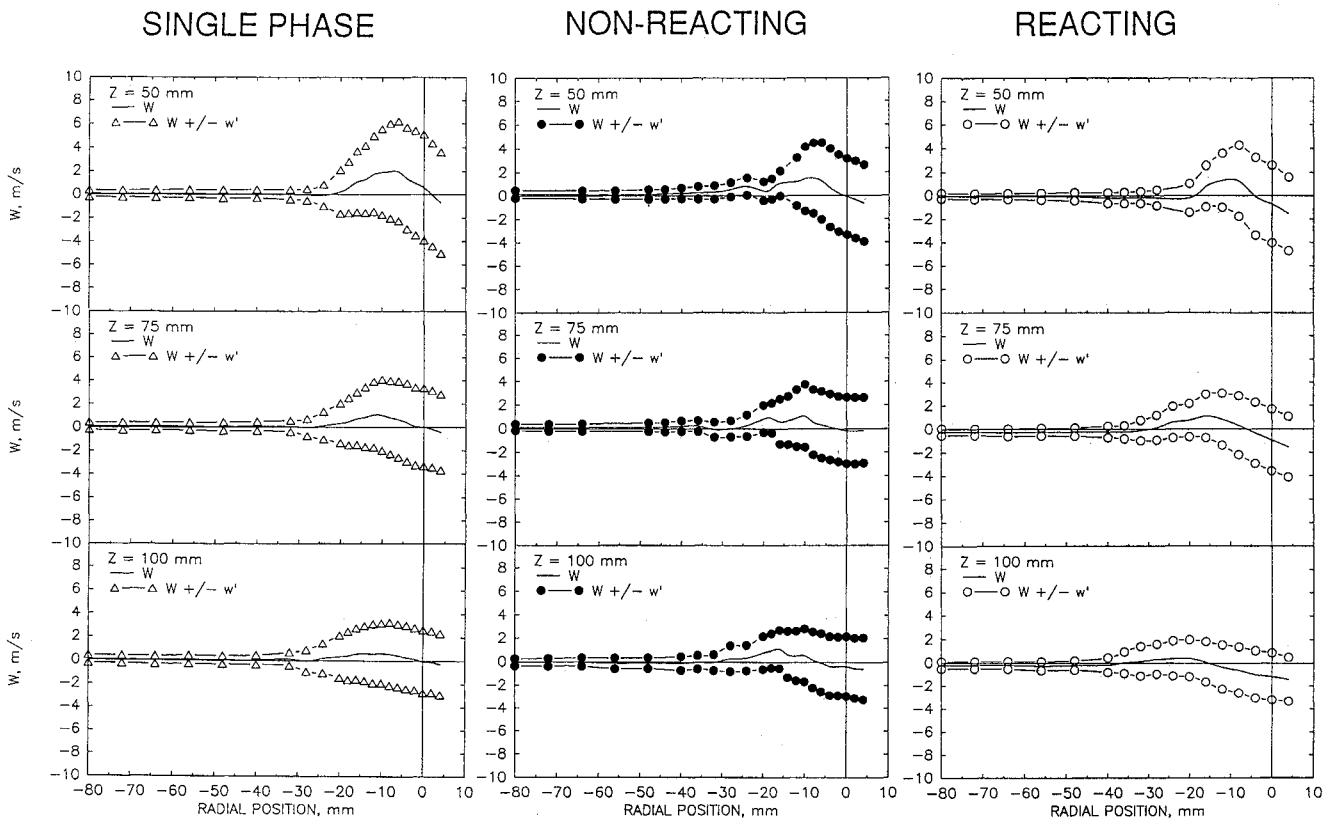


**Fig. 6 Continuous phase azimuthal velocities.**

eral, and the particular test article employed in this study are prone to asymmetries under the scrutiny of the advanced diagnostic techniques now available.[16] Based on previous symmetry assessments of the atomizer used in the present study, the shift in the centerline is attributed to an asymmetric heat release associated with an asymmetry in the fuel distribution.[9]

The fluctuating azimuthal velocities exhibit trends similar to those observed for the axial direction. The fluctuating azimuthal velocities tend to be lower than the axial values for all three cases. To illustrate this, Fig. 7 presents radial profiles at $Z = 100$ mm of the ratio of the fluctuating azimuthal velocity to the fluctuating axial velocity. The presence of the

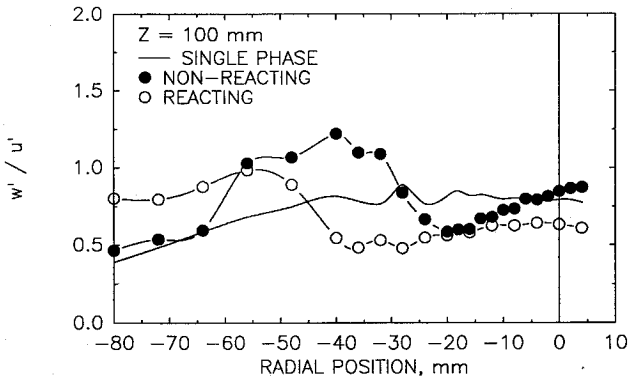


**Fig. 7 Radial profile of $w'/u'$ at $Z = 100$ mm.**

drops increases the isotropy at the edge of the spray (i.e., $u'/w' \approx 1$). However, the level of isotropy is decreased by the presence of the reacting spray at all locations, except those farthest from the centerline. This is attributed to the strong acceleration of the gases in the axial direction, coupled with little acceleration in the azimuthal direction.

**Dispersed Phase**

At this point, it is useful to examine the physical structure of the spray in terms of where and for how long drops exist. Application of group combustion theory proposed by Chiu[17] yields a group combustion number, $G >> 10^2$, indicating that evaporation of drops should occur within a sheath of flame. The presence of a sheath flame is noticed to some extent, although droplets are clearly present outside of the flame sheath.

The droplet burning time can be estimated from Spalding[18] as being $D_o^2 \times 10^{-6}$, where $D_o$ is the initial droplet diameter. This leads to typical burning times of 0.1 ms for 10 $\mu$m and 10 ms for 100 $\mu$m drops. Given the velocities for these drops (generally less than 20 m/s in the reaction zone), it is evident that small drops will not penetrate far into the reacting region. Even 100 $\mu$m drops can travel only 100–150 mm into the reaction zone.

This discussion is consistent with the observed structure of the spray—a relatively dense droplet core is surrounded by an annular reaction zone with complete droplet burn out by $Z = 125$ mm. A primary exception is the presence of drops outside the flame sheath, which is attributed to 1) the formation and injection of unusually large droplets (i.e., "rogue droplets") with high radial velocities, and 2) the dynamics associated with the flame and trajectories of drops. With this perspective, discussion of the in-situ droplet measurements follow.

*Droplet Distribution $D_{10}$ and $D_{32}$*

Figure 8 presents radial profiles of the droplet distribution number mean ($D_{10}$) and Sauter mean ($D_{32}$) diameters for the reacting and non-reacting sprays. The means are based upon the corrected size distribution resulting from compensation for variation of sample volume with drop size.[12] At $Z = 50$ mm, $D_{32}$ is unchanged by reaction, indicating that the largest drops (which have the strongest influence on $D_{32}$) have enough thermal inertia to avoid significant reduction in diameter. At the centerline, $D_{10}$ is systematically larger for the reacting case, but the difference observed is within experimental error.

At $Z = 75$ and 100 mm, both $D_{10}$ and $D_{32}$ are reduced significantly at the outer edge of the spray under reacting conditions. At $Z = 75$ mm, $D_{32}$ for each case is the same at centerline, indicating that the largest drops there are unaffected by the heat release. Changes in $D_{10}$ remain within experimental error. At $Z = 100$ mm, $D_{32}$ for the reacting case is smaller at radial locations, indicating that even the largest drops are reduced in size, due to heat release.

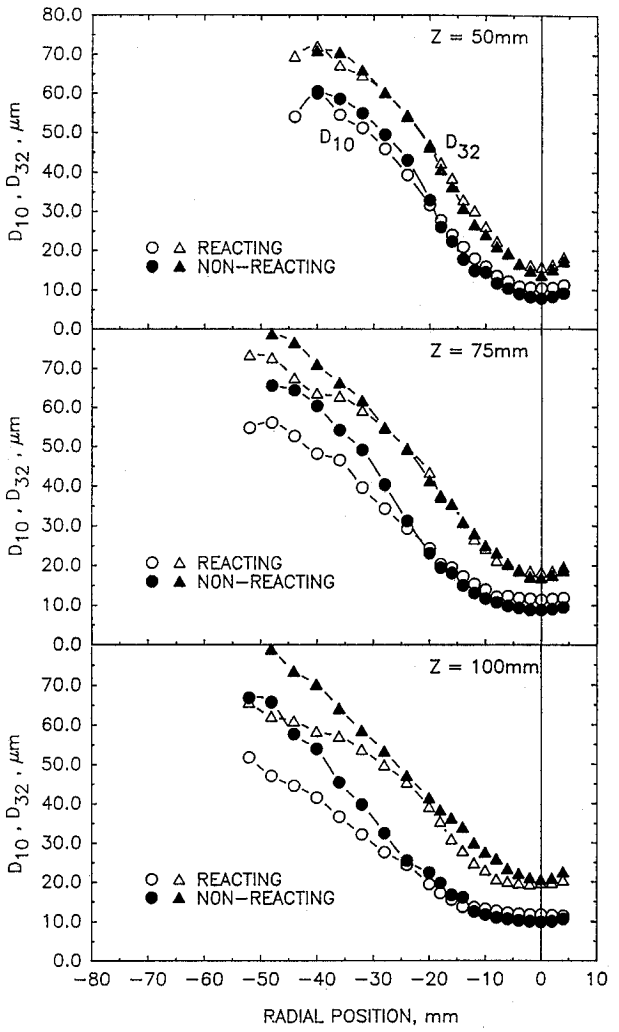


**Fig. 8 Droplet distribution $D_{10}$ and $D_{32}$ profiles.**

*Droplet Volume Distribution Span*

Figure 9 presents radial profile of the span of the droplet volume distribution for the two cases. The span is defined as $D_{0.9}-D_{0.1}$, where $D_{0.1}$ and $D_{0.9}$ are the diameters at which 10% and 90% of the volume in the distribution lies below, respectively. At $Z = 50$ mm, little difference is observed between the two cases, which is consistent with the previous discussion. At $Z = 75$ mm and $Z = 100$ mm, a substantial increase in the span is observed for the reacting case within the region of the reaction zone. This is associated with an increase in the $D_{0.9}$ value, as well as a decrease in the $D_{0.1}$ value. By way of explanation, the smallest, most numerous drops rapidly disappear as a result of evaporation. This results in a larger $D_{0.9}$ value. However, at the same time, medium-sized drops vaporize, "replacing" the small-drop population to such an extent that the $D_{0.1}$ value is also reduced. The net result is that the volume of the distribution is represented by a much larger range of drop sizes, resulting in a larger span value for the reacting case. Note that, even though the distribution $D_{10}$ and $D_{32}$ values do not change significantly, the shape of the volume (and count) distributions change markedly. This illustrates the importance of measuring the droplet size distribution.

*Droplet Volume Flux*

Figure 10 presents radial profiles of local volume flux (volume of liquid passing through the interferometric probe volume cross section per unit time) in the spray, under reacting and non-reacting conditions. At $Z = 50$ mm, the profiles are similar, as expected. At $Z = 75$ mm, considerable reduction

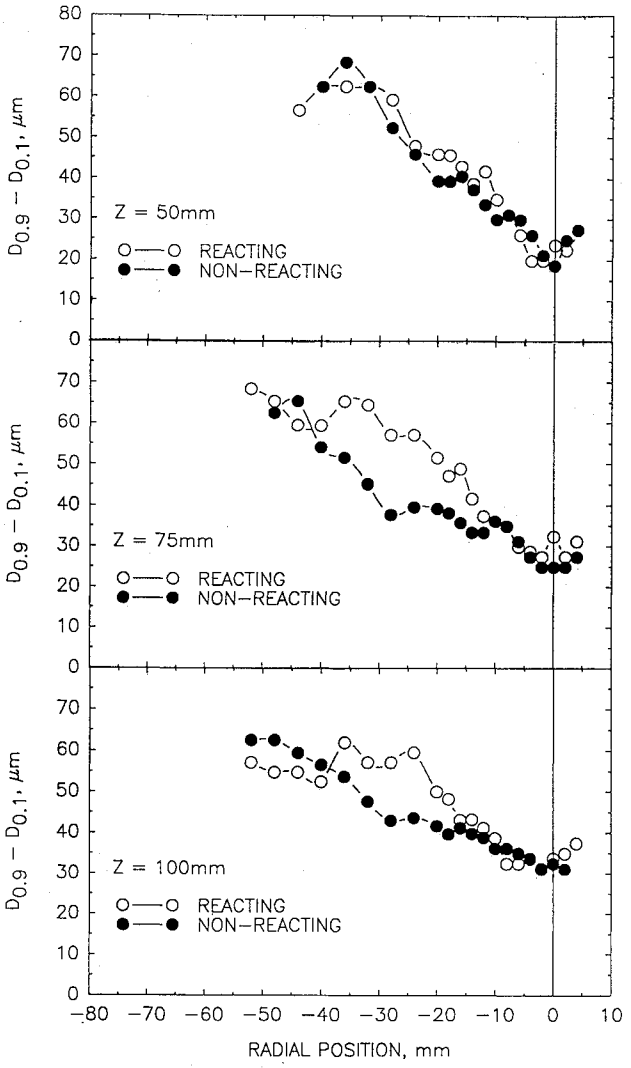


**Fig. 9 Span of the droplet volume distribution.**

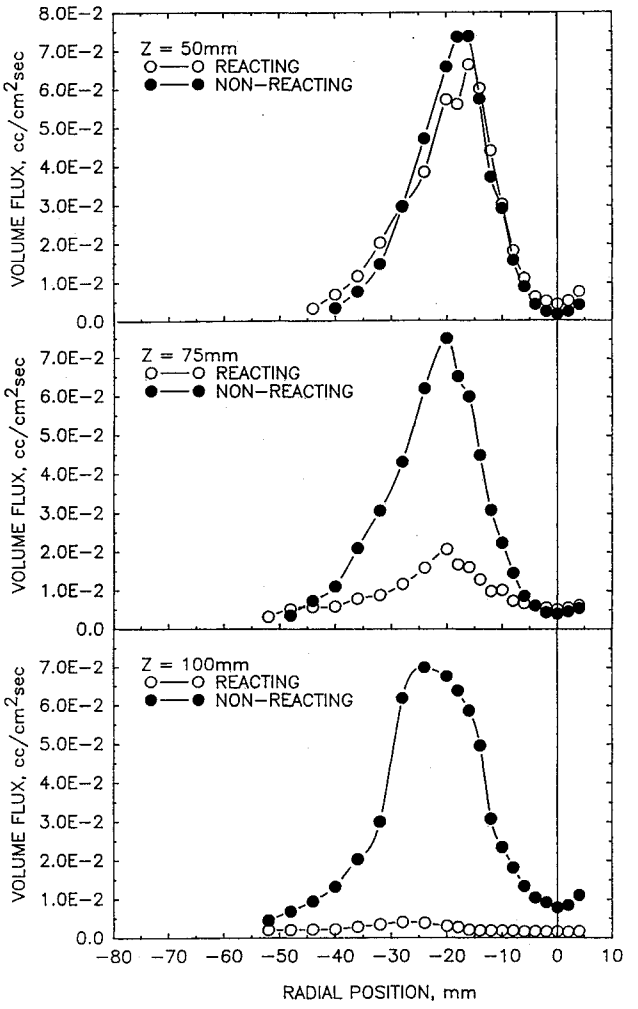


**Fig. 10 Droplet volume flux.**

in volume flux in the reacting spray has occurred. By $Z$ = 100 mm, nearly all the droplets have evaporated in the reacting case, whereas the non-reacting profile shows a reduction in the peak value and increased radial spread of the spray due to dispersion of the drops.

To assess the ability of the instrument to measure volume flux accurately, the previous radial profiles of volume flux were integrated over the radial and azimuthal directions to give a value of the volumetric flow rate. Figure 11 presents the axial variation in volume flow rate for the reacting and non-reacting cases. At $Z$ = 50 mm, the volume flow rate is about 60% of the injected value. This difference between the injected and measured volume flux is reduced by $Z$ = 75 mm, and at $Z$ = 100 mm, reasonable conservation of volume is reached, especially if evaporation is accounted for.

Several factors contribute to the low value at $Z$ = 50 mm. The high axial velocities cause droplets to be missed, due to insufficient frequency shift in the azimuthal component (i.e., fringe biasing). Also, the high absolute data rates (>3000 Hz) can cause excess rejection of sources, due to multiple particles in the probe volume. The rejected drops are not used in the calculation of the flux. In the present study, rejection rates ranged from 5 to 60%, depending on the location in the spray. In general, the highest rejection rates occurred only nearest to the atomizer and at the center of the spray. This problem may be reduced by using a smaller spatial filter in the receiver, but cannot be eliminated. In addition, asymmetry of the atomizer will contribute to errors.[9]

*Droplet Velocities*

Figure 12 presents mean axial velocities for selected droplet size groups. Group widths were selected to provide a wide range of areas over which a statistically representative number of droplets were present. (Data are presented only for locations at which more than 100 drops of a given size range were measured.)

At $Z$ = 50 mm, the profiles, with the exception of slightly higher axial velocities, are similar for both reacting and non-reacting cases. At $Z$ = 75 mm, a dependency of velocity on size is more persistent in the reacting case. This persistence is even more evident at $Z$ = 100 mm.

One reason for the persistence of the size-velocity correlation in the reacting case is that the drops present at $Z$ = 100 mm were considerably larger when they were at $Z$ = 50 mm. For example, applying the $d$-squared law[18] to drops present at $Z$ = 100 mm indicates that the drop must be 57$\mu$m in diameter at $Z$ = 50 mm (assuming a velocity of 15 m/s). Hence, drops of a given size present at $Z$ = 100 mm in the reacting case were larger drops with more momentum at $Z$ = 50 mm, whereas drops of a given size present at $Z$ = 100 mm in the non-reacting case were similar in size at $Z$ = 50 mm.

In addition, the persistence of the size-velocity correlation may be partially due to a reduction in drag force on the droplets. It has been shown by some researchers (e.g., Refs. 19 and 20) that evaporative blowing and influence of the boundary layer on the effective viscosity can reduce the total drag on drops (especially low-temperature drops) injected into a high-temperature environment. This situation is likely to exist in the present case, and it could be that these phe-

nomena are occurring as well. Without the luxury of a Lagrangian measurement, the presence of such effects cannot be established.

The droplet azimuthal velocities (not presented here, for brevity) demonstrate no significant velocity dependency upon size, indicating little momentum transfer between phases associated with this component of velocity.

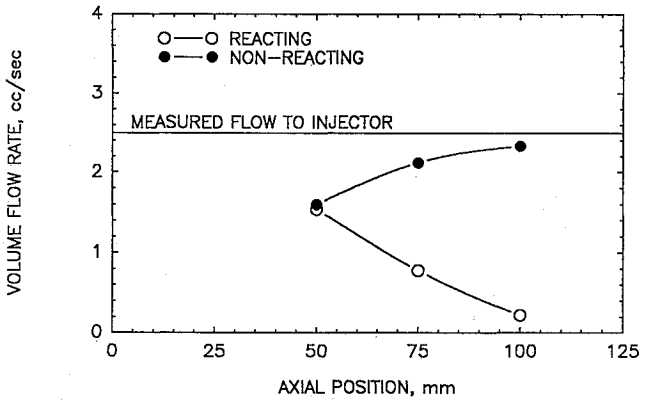


**Fig. 11 Axial variation in integrated volume flux.**

Fluctuating droplet velocities are not presented because of the ambiguity associated with the "smearing" of this quantity, due to size velocity correlations within the size group, and the inability to distinguish where drops at a given point came from. It is noted that the variation in droplet velocity plays a role in the dispersion of drops, and may impact correlation with empirical relationships. Efforts are currently being directed at better understanding the role of the fluctuating drop velocities.

## Summary

A detailed study of the flow produced by an air-blast atomizer operated with no liquid and liquid under reacting and non-reacting conditions is conducted. Spatially resolved measurements of the axial and azimuthal components of velocity for each phase are obtained, as well as droplet size distributions and volume flux. In summary, for the test article and operating conditions evaluated:

1) Quantification of the air flow splits through the atomizer and the way in which the presence of the liquid impacted the gas injection velocity was necessary to properly interpret the data.

2) The presence of the drops under non-reacting conditions increases the continuous-phase mean axial velocities, reduces

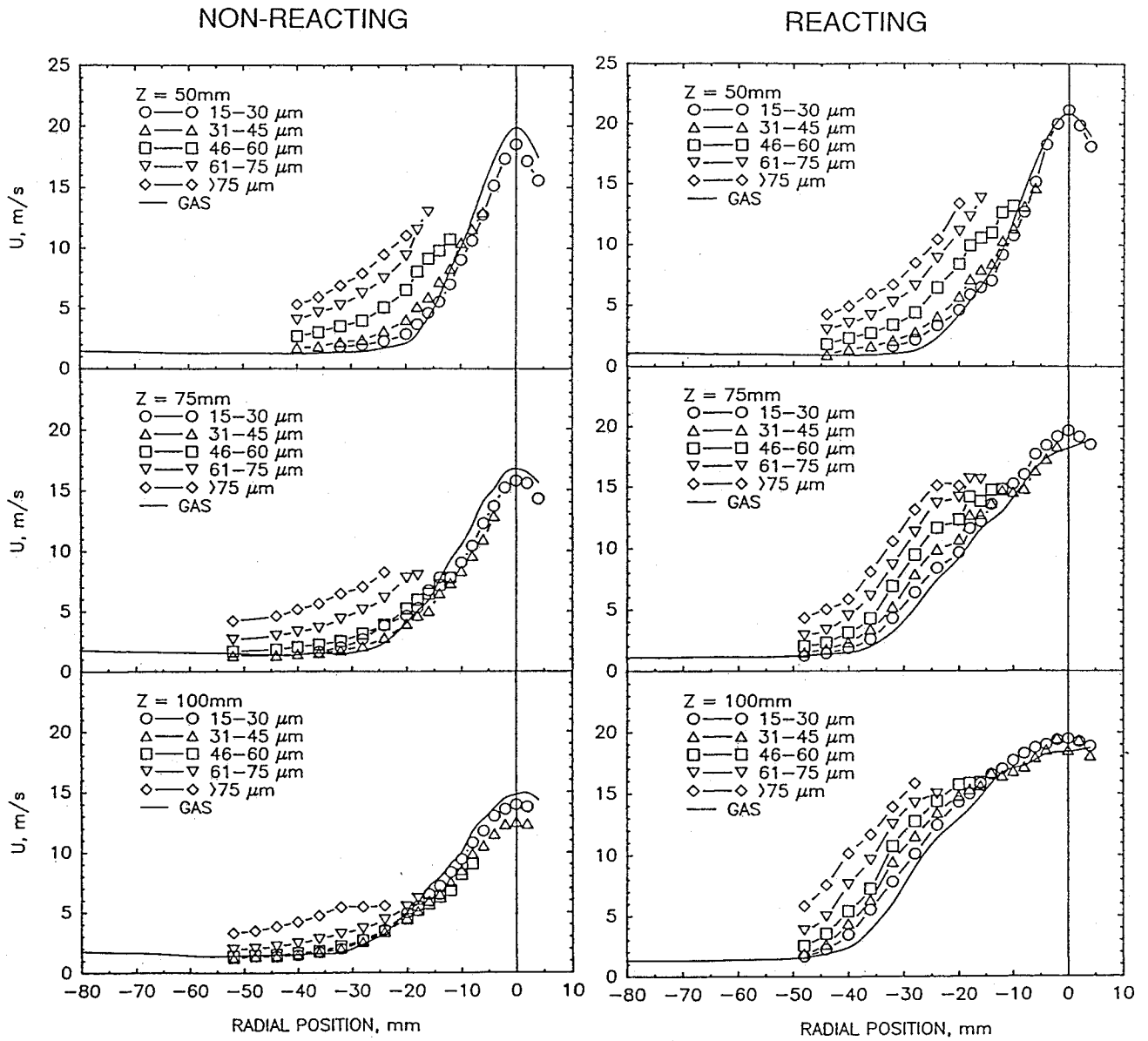


**Fig. 12 Droplet mean axial velocities.**

turbulence in the continuous phase, and slows the decay of the continuous phase velocities relative to the single-phase case. This is attributed to a combination of momentum transfer between phases, and to changes in the inlet condition of the atomizer between the single and two-phase cases.

3) The single and two-phase flows both exhibit anistropy. The degree of anisotropy is increased by reaction.

4) Reaction increases the gas phase mean and fluctuating axial velocities.

5) Reaction reduces the local volume flux and size distribution means.

6) Reaction increases the span of the volume distribution, which is attributed to preferential evaporation of small drops.

7) Reaction causes a persistence of a drop size-axial velocity correlation, which is attributed to differences in the evaporative history of drops between the reacting and non-reacting cases.

8) The general structure of the present spray flame is consistent with group combustion theory, although it is noted that individual ("rogue") drops still exist outside of the reaction zone.

9) The lifetime of droplets in the flame is described with reasonable accuracy by the $D^2$ law.

This study provides a data base for air-blast atomizers that can be used to investigate the performance of numerical models in predicting droplet/gas behavior in reacting sprays.

## Acknowledgments

This work was supported, in part, by NASA Contract NAS3-24350 (J. D. Holdeman, contract monitor) in cooperation with the Allison Gas Turbine Division of General Motors. Facility support from Howard Crum is greatly appreciated. The participation of Chris Brown in the collection of the data is gratefully acknowledged. Also, the help of Greg Hill in development of data reduction software is appreciated.

## References

[1]Cameron, C. D., Brouwer, J., and Samuelsen, G. S., "A Model Gas Turbine Combustor With Wall Jets and Optical Access for Turbulent Mixing, Fuel Effects, and Spray Studies," *Twenty-Second Symposium (International) on Combustion*, The Combustion Inst., Pittsburgh, PA, 1988, pp. 465–474.

[2]McDonell, V. G., Wood, C. P., and Samuelsen, G. S., "A Comparison of Spatially-Resolved Drop Size and Drop Velocity Measurements in an Isothermal Chamber and a Swirl-Stabilized Combustor," *Twenty-First Symposium (International) on Combustion*, The Combustion Inst., Pittsburgh, PA, 1986, pp. 685–694.

[3]Mao, C.-P., Wang, G., and Chigier, N. A., "An Experimental Study of Air-Assist Atomizer Spray Flames," *Twenty-First Symposium (International) on Combustion*, The Combustion Inst., Pittsburgh, PA, 1986, pp. 665–673.

[4]Presser, C., Gupta, A. K., Semerjian, H. G., and Santoro, R. J., "Droplet/air Interaction in a Swirl-Stabilized Spray Flames," *Proceedings of the 2nd ASME/JSME Thermal Engineering Joint Conf.*, Vol. 1, 1987, pp. 73–83.

[5]McDonell, V. G., and Samuelsen, G. S., "Application of Two-Component Phase Doppler Interferometry to the Measurement of Particle Size, Mass Flux, and Velocities in Two-phase Flows," *Twenty-Second Symposium (International) on Combustion*, The Combustion Inst., Pittsburgh, PA, 1988, pp. 1961–1971.

[6]Mostafa, A. A., Mongia, H. C., McDonell, V. G., and Samuelsen, G. S., "On the Evolution of Particle-Laden Jet Flows: a Theoretical and Experimental Study," *AIAA Journal*, Vol. 27, No. 2, 1989, pp. 167–183.

[7]Bulzan, D. L., "Particle-Laden Weakly Swirling Free Jets: Measurements and Predictions," NASA TM-100881 May 1987.

[8]Breña de la Rosa, A., Bachalo, W. D., and Rudoff, R. C., "Spray Characterization and Turbulence Properties in an Isothermal Spray with Swirl," *ASME Journal of Engineering for Gas Turbines and Power*, Vol. 112, No. 1, 1990, pp. 61–66.

[9]McDonell, V. G., and Samuelsen, G. S., "Influence of Continuous and Dispersed Phases on the Symmetry of a Gas-Turbine Air-Blast Atomizer," *ASME Journal of Engineering for Gas Turbines and Power*, Vol. 112, No. 1, 1990, pp. 44–51.

[10]McDonell, V. G., and Samuelsen, G. S., "Evolution of the Two-Phase Flow in the Near Field of an Air-Blast Atomizer Under Reacting and Non-Reacting Conditions," in *Applications of Laser Anemometry to Fluid Mechanics (4th International Symposium)*. Adrian, R. J., Asanuma, T., Durão, D. F. G, Durst, F., and Whitelaw, J. H. (eds.), Springer-Verlag, London, England, 1989, pp. 255–278.

[11]Koblish, T., private communication.

[12]Bachalo, W. D., and Houser, M. J., "Phase Doppler Spray Analyzer for the Simultaneous Measurement of Droplet Size and Velocity," *Optical Engineering*, Vol. 23, No. 5, 1984, pp. 583–590.

[13]Bachalo, W. D., Rudoff, R. C., and Breña de la Rosa, A., "Mass Flux Measurements of a High Number Density Spray System Using the Phase Doppler Spray Analyzer," AIAA Paper No. 88-0236, Jan. 1988.

[14]McDonell, V. G., and Samuelsen, G. S., "Optical Measurements of the Behavior of a Polydispersed Spray Under Reacting and Non-reacting Conditions," WSS Paper No. 89-59, presented at WSS/CI Fall Meeting, Livermore, CA.

[15]McVey, J. B., Kennedy, J. B., and Russell, S., "Application of Advanced Diagnostics to Airblast Injector Flows," *ASME Journal for Gas Turbines and Power*, Vol. 111, No. 1, 1989, pp. 53–62.

[16]McDonell, V. G., Cameron, C. D., and Samuelsen, G. S., "Symmetry Assessment of an Air-Blast Atomizer Spray," *Journal of Propulsion and Power*, Vol. 6, No. 4, July–Aug. 1990, pp. 375–381.

[17]Chiu, H. H., and Liu, T. M., "Group Combustion of Liquid Droplets," *Combustion Science and Technology*, Vol. 17, 1977, pp. 127–142.

[18]Spalding, D. B., *Combustion and Mass Transfer*, Pergamon Press, Oxford, England, UK 1979.

[19]Dwyer, H. A., and Sanders, B. R., "A Detailed Study of Burning Fuel Droplets," *Twenty-First Symposium (International) on Combustion*, The Combustion Inst., Pittsburgh, PA, 1986, pp. 633–639.

[20]Dukowicz, J. K., "Drag of Evaporating or Condensing Droplets in Low Reynolds Number Flow," *Physics of Fluids*, Vol. 27, No. 6, 1984, pp. 1351–1358.